

Organoplatinum Chromophores for Application in High-Performance Nonlinear Absorption Materials

Chen Liao, Abigail H. Shelton, Kye-Young Kim, and Kirk S. Schanze*

Department of Chemistry and Center for Macromolecular Science and Engineering, University of Florida, P.O. Box 117200, Gainesville, Florida 32611, United States

ABSTRACT:



Chromophores and materials that exhibit nonlinear absorption over a broad spectrum and with high temporal dynamic range are of interest for application in materials engineering and biology. Recent work by a number of research groups has led to the development of a new family of organometallic chromophores and materials featuring interesting and useful nonlinear absorption properties. These systems contain the platinum acetylide moiety as a fundamental molecular unit, combined with delocalized, π -conjugated electron systems. These organometallic chromophores provide a unique combination of properties, such as negligible ground state absorption in the visible region, large spin–orbit coupling giving rise to high triplet excited state yield, triplet lifetime in the microsecond domain, high two-photon cross-section in the visible and near-infrared regions, and high triplet–triplet absorption cross-section in the visible and near-infrared region. This Spotlight on Application highlights recent developments in this area, combining background and review on nonlinear absorption in platinum acetylide chromophores and describing significant recent results from our own laboratory.

KEYWORDS: platinum acetylide, nonlinear absorption, two-photon absorption, reverse saturable absorption

INTRODUCTION

Over the last two decades, there has been significant interest in the study of π -conjugated molecules because of their potential for use in electronic and optoelectronic applications. For example, interest in conjugated materials derives from applications such as optical data storage,^{1,2} optical limiting,³ photovoltaic devices,⁴ three-dimensional microfabrication,⁵ microscopy,⁶ and photodynamic therapy.⁷ This Spotlight on Applications is focused on platinum acetylide-based π -conjugated materials with applications to nonlinear absorption (NLA). These unique organic–inorganic hybrid materials feature a π -conjugated organic framework that is strongly coupled to platinum(II) centers via overlap of the organic π -electron system with metal centered d-orbitals of appropriate symmetry. The design, synthesis, unique one-photon and two-photon photophysical properties, and materials properties of platinum acetylides will be explored within this Spotlight.

Platinum acetylide complexes and polymers feature a four coordinate, square planar platinum(II) center with the general formula $\text{PtL}_2(\text{C}\equiv\text{CR}')_2$, where L is typically a phosphine ligand (PR_3) and $\text{C}\equiv\text{CR}'$ is an aryl acetylide unit (i.e., $\text{R}' = \text{aryl}$). Though most investigations center on platinum acetylides having the trans configuration at the platinum center (*trans*- $\text{Pt}(\text{PR}_3)_2(\text{C}\equiv\text{CR}')_2$), aryl acetylide moieties have been incorporated onto the platinum metal center in the cis configuration as well.⁸ The

alkyl (R) groups on the phosphine ligands are typically aliphatic, and they contribute to the materials properties of the complex or polymer (e.g., degree of crystallinity, melting point, solubility, etc.). In general, R' is a π -conjugated aromatic group that dominates the photophysical properties of the complex or polymer; common are phenylene,⁹ thienylene,¹⁰ and fluorenylene¹¹ groups. Incorporation of the platinum(II) center into organic chromophores leads to high yield of the triplet excited state, and it can also influence the redox and optoelectronic properties of the complex or polymer; often the effects of the metal center and the organic structures can be predicted, allowing systematic variation and tuning of these properties.

Platinum acetylides often display high linear transmission throughout most of the visible region.¹² Because the platinum center has a propensity to mix the triplet and singlet excited state manifolds by spin–orbit coupling, there is an opportunity for examination of spin-forbidden absorption from the singlet ground state to the triplet excited state ($S_0 + h\nu \rightarrow T_1$), intersystem crossing (ISC) of singlet to triplet excited state ($S_1 \rightarrow T_1$), triplet state phosphorescence emission ($T_1 \rightarrow S_0 + h\nu$), and triplet–triplet excited state absorption ($T_1 + h\nu \rightarrow T_n$).

Received: April 19, 2011

Accepted: May 31, 2011

Published: May 31, 2011

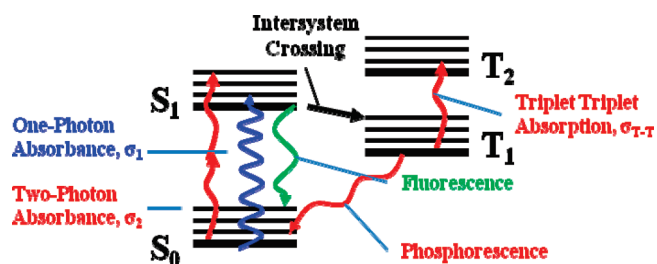


Figure 1. Jablonski diagram for a typical chromophore that exhibits two-photon absorption, intersystem crossing, and triplet–triplet absorption.

These materials, as will be discussed, are also ideal candidates for enhanced NLA over the visible and near-infrared spectral region.^{12,13}

Two-Photon Absorption. A brief discussion of two-photon absorption (2PA) mechanisms is introduced here before presenting the enhanced NLA mechanisms that operate in platinum acetylide chromophores. Two-photon absorption is the simultaneous absorption of two photons resulting in the excitation of a chromophore from the ground state to an electronic excited state (Figure 1). If the two photons are of the same wavelength, this process is referred as degenerate 2PA. The energy difference between the lower and upper states is equal to the sum of the energies of the two photons. Compared to conventional one-photon absorption, the 2PA process is advantageous for nonlinear absorption application for several reasons. First, 2PA has an instantaneous response time (<1 ps), it depends on temporal overlap of the two photons, and it shows a quadratic dependence on light intensity ($2PA \propto I^2$); consequently, a 2PA-induced photochemical processes usually occurs in a small focal region. Furthermore, the 2PA-absorbing material is often protected from photodegradation effects through the use of two lower-energy photons instead of the one higher-energy photon in linear one-photon absorption (1PA) pathways. Chromophores that exhibit 2PA, and the ensuing fundamental properties and application possibilities, have been extensively studied and reviewed in recent years.^{11–19} For example, in the rather extensive review by He et al.,¹⁵ 2PA dyes can be grouped into organic molecules, liquid crystals, conjugated polymers, fullerenes, coordination and organometallic compounds, porphyrins and metalloporphyrins, nanoparticles, and biomolecules and derivatives.

Since the two-photon absorption cross-section (σ_2) of a typical platinum acetylide chromophore is relatively small (on the order of 1 GM, where $1 \text{ GM} = 1 \times 10^{-50} \text{ cm}^4 \text{ s photon}^{-1}$), research on these systems has focused on improving σ_2 which is a fundamentally important parameter that needs to be optimized for practical application in nonlinear absorption. When one considers designing highly effective 2PA chromophores, the general guideline typically involves several paradigms such as (1) extended conjugation length with planar chromophores; (2) motifs such as $D-\pi-D$, $A-\pi-A$, and $D-\pi-A$ (where $D = \text{donor}$, $A = \text{acceptor}$ and $\pi = \text{conjugated spacer}$); (3) increasing the π -donor or π -acceptor strength; (4) introduction of more polarizable unsaturated bonds; and (5) variation in the nature of the conjugated bridge.^{20,21} As such, the design, synthesis and fabrication, and structure–property relationships of platinum acetylide NLA chromophores has been considered within these design criteria for effective 2PA chromophores.

Reverse Saturable Absorption. In addition to 2PA, reverse saturable absorption (RSA) is another NLA pathway available for

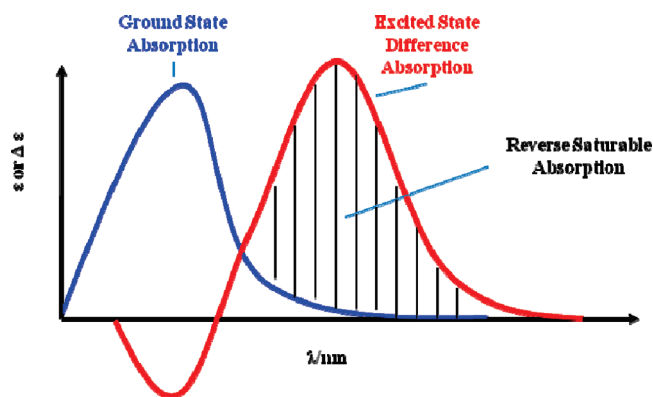


Figure 2. Schematic illustrating idealized ground-state and excited-state difference absorption spectra for a chromophore that exhibits reverse saturable absorption.

chromophores that have a small, nonzero ground-state absorption cross-section (σ_1) over a specific spectral region and a large excited-state absorption (ESA) cross-section (σ_{ESA}) in the same wavelength region.²⁰ The excited state absorption can originate from all possible transient states, most often the lowest-energy singlet and triplet excited states. Generally, as the light intensity increases, the population of the singlet and triplet excited states increases. In RSA, the excited state exhibits more absorption than the ground state, resulting in more absorption as the incident optical flux increases. The magnitude of RSA is proportional to the ratio $\sigma_{\text{ESA}}/\sigma_1$, and the larger the ratio, the stronger the RSA. Figure 2 illustrates the singlet ground state absorption and triplet ESA of an arbitrary molecule that could exhibit RSA. RSA is observed in a variety of chromophores, including porphyrins, indanthrones, metal cluster compounds, fullerenes, cyanines, phthalocyanines, and naphthalocyanines, as reviewed by Perry.²²

Combined Two-Photon Absorption and Excited-State Absorption. In some molecular and polymer systems, it is possible to observe nonlinear absorption because of a combination of instantaneous multiphoton absorption by the 2PA mechanism, followed by subsequent excited-state absorption (ESA) due to a strongly absorbing excited state produced by the initial 2PA excitation. This process, which we refer to as the 2PA/ESA dual mechanism, can be understood by reference to the Jablonski diagram in Figure 1. Both simultaneous 2PA (efficiency determined by σ_2) and 1PA (efficiency determined by σ_1) can populate the singlet excited state $S_0 \rightarrow S_1$. Because the selection rules for 2PA and 1PA are different,²³ usually the 2PA-induced singlet state lies at a slightly higher energy than 1PA-induced excited state for a centrosymmetric compound.¹⁴ Platinum, like other heavy transition metals, efficiently mixes the singlet and triplet excited states via spin–orbit coupling, resulting in a rapid and efficient $S_1 \rightarrow T_1$ ISC ($\Phi_{\text{ISC}} > 90\%$) to populate the triplet excited state T_1 . Excited state absorption due to the strongly allowed $T_1 \rightarrow T_n$ transition then occurs after the triplet population builds up (in the 10–400 ps time scale).^{24,25} The combined 2PA/ESA mechanism gives rise to an overall nonlinear response in the fs–ns time scale^{22,26} because 2PA occurs instantaneously (fs–ps), and then the triplet state is produced by ISC and persists into the ns– μs time scale.²⁴ As will be discussed, nonlinear absorption via 2PA/ESA is most efficient in chromophores where the 2PA absorption maximum coincides spectrally with ESA.²⁷

As we will discuss below, in some platinum acetylides the 2PA/ESA dual mechanism is effective, affording these materials with

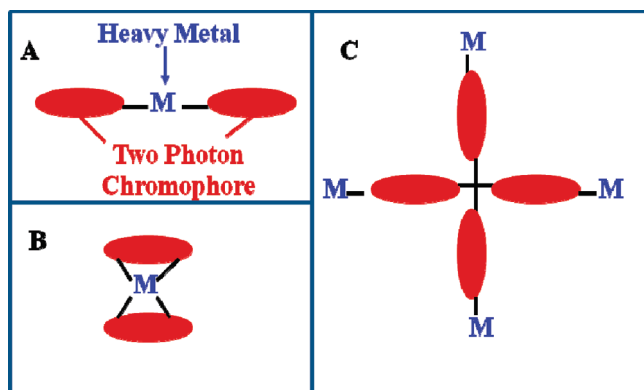


Figure 3. Cartoons illustrating design motifs for organometallic 2PA/ESA chromophores.

broad temporal and broad frequency NLA response in the region of 500–800 nm.^{24,25} The ultraviolet and blue region (<500 nm) consists of one-photon excitation to the singlet excited state followed by rapid ISC to the triplet excited state. The green region ($\lambda_{\text{ex}} = 500\text{--}570$ nm) exhibits direct spin-forbidden excitation of the triplet excited state from the singlet ground state ($S_0 \rightarrow T_1$) that can be occasionally observed in platinum acetylides, as well as the triplet–triplet absorption.²⁴ The yellow and red wavelength region ($\lambda_{\text{ex}} = 540\text{--}700$ nm) is dominated by strong 2PA to populate the singlet excited state, followed by rapid ISC to the triplet excited state, which is also highly absorbing throughout the region of 600–800 nm for most platinum acetylide chromophores.

Structural Motif for Organometallic NLA Chromophores. Efficient nonlinear absorption via organometallic 2PA/ESA complexes is often achieved through one of a few well-defined general chromophore motifs, as illustrated in Figure 3.

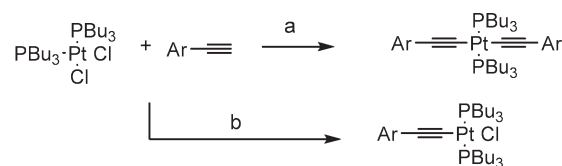
In platinum acetylide systems, the metal–carbon bond (Pt–C) links the Pt center and the acetylene unit, and the complexes are comparatively stable due to $d\pi\text{--}p\pi$ overlap. In other motifs, the platinum center can bond to two chromophoric ligands as suggested in A and B (Figure 3) giving rise to a linear two-dimensional or a three-dimensional coordination scaffold, or it can act as an “end-cap” functionalization unit (as suggested in C). The acetylide ligand is typically an extended π -conjugated chromophore with strong electron-donating or electron-withdrawing capability.²⁸

Objective and Scope of Spotlight Article. The objective of this Spotlight article is to provide an overall perspective and review of recent developments and directions in the platinum acetylide chromophores and polymers developed for application as high performance nonlinear absorption materials. This article is not intended to be an exhaustive review, and in some cases previously unpublished work from the authors’ recent work is included. The reader is directed to other recent authoritative reviews for different perspectives on this class of materials and NLA applications.^{13,29–31}

PLATINUM ACETYLIDE COMPLEXES AND POLYMERS: SYNTHESIS AND STRUCTURES

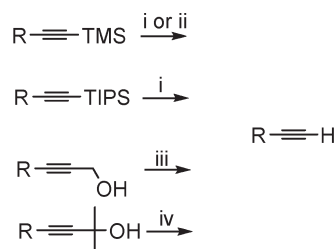
Synthesis of Platinum Acetylides. There are a number of synthetic methods for generating platinum acetylide complexes. The first series of platinum acetylides were prepared by a copper(I) halide catalyzed dehydrohalogenation reaction between *cis*-

Scheme 1. Hagihara Coupling of *cis*-Pt(PBu₃)₂Cl₂ and Acetylene



^a(a) CuI, diethylamine; (b) Reflux, diethylamine.

Scheme 2. Protecting Group Strategies for Terminal Acetylides



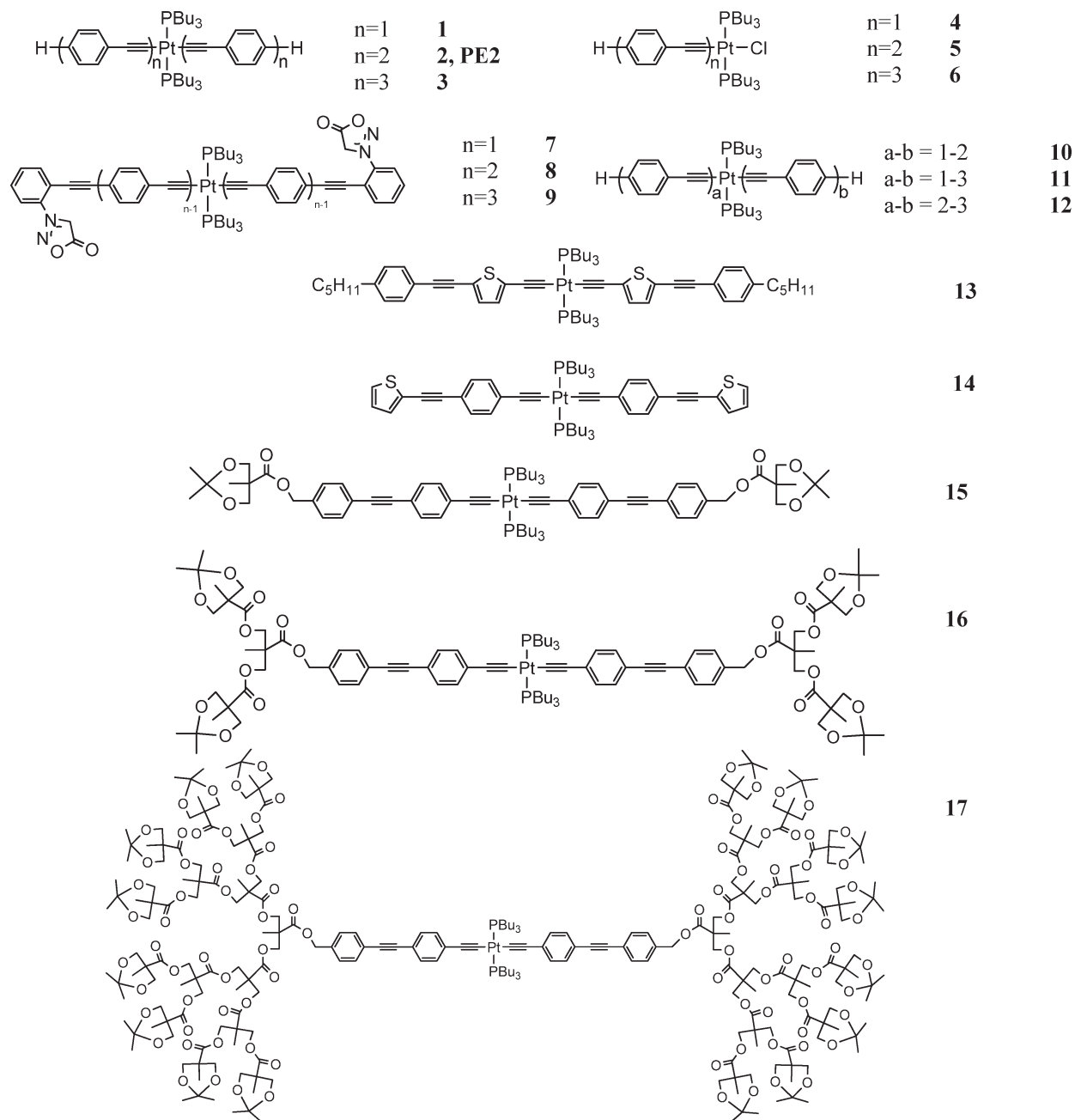
i). TBAF, rt, ii). K₂CO₃, MeOH/CH₂Cl₂, rt, 1h, iii) MnO₂, KOH, Et₂O, rt, iv) Benzene, NaOH, reflux 12h.

trans-Pt(PBu₃)₂Cl₂ and terminal alkynes in alkylamine, as reported by Hagihara, Sonogashira, and co-workers.³² The reactions proceeded under mild conditions, generating dialkynyl Pt(II) complexes with yields above 80%, as shown in route a (Scheme 1). Efficient synthesis of monoalkynyl platinum(II) complexes is possible through the direct reaction between *cis*-Pt(PPh₃)₂Cl₂ and a terminal acetylene in the absence of copper(I) halide, as shown in route b (Scheme 1).^{33,34}

Several variations on these synthetic protocols have been explored. Efficient one-pot synthesis of *trans* mono- or dialkynyl platinum(II) complexes has been reported by heating PtCl₂, alkyne, and trialkylphosphine in tetrahydrofuran and triethylamine.³⁵ Organotin compounds have been reported by Lewis and co-workers to afford the dialkynyl platinum complexes via a transmetalation reaction with *trans*-Pt(PBu₃)₂Cl₂.^{36,37} Oligomers and polymers can also be synthesized by dehydrohalogenation reaction between equivalent amounts of *cis*-Pt(PBu₃)₂Cl₂ and bis-terminal acetylides in the presence of CuI and amine.^{38,39}

Conjugated oligomers with precise length and constitution can be synthesized by employing either a fractionation growth or a step-growth method.^{40,41} By using orthogonal protective groups that can be selectively deprotected (Scheme 2),⁴² together with iterative/iterative-convergent coupling reactions, it is possible to generate structurally well-defined platinum acetylide oligomers.^{43–46} For example, we reported the synthesis of a series of monodisperse platinum acetylides end-capped by naphthalene diimide units (NDI) using the iterative convergent method, generating the structures NDI–[Ph–C≡C–Pt(PBu₃)₂–C≡C–]_n–Ph–NDI, where $n = 2, 3, 6, \text{ or } 10$; Ph is 1,4-phenylene; and NDI is a substituted 1,4,5,8-naphthalene diimide.⁴⁴ Tetrahedral star-shaped branched platinum acetylide oligomers⁴⁷ and platinum acetylide dendrimers up to the third generation with tri- and tetra-functional cores⁴⁸ have also been

Chart 1. Phenylene-ethynylene Platinum Acetylide Chromophores



generated in a similar fashion, illustrating the versatility of the coupling reactions to generate diverse platinum acetylide materials.

Diverse Structures of Platinum Acetylides. The synthetic techniques discussed above have been utilized for synthesizing many platinum acetylide compounds with diverse functionality, chromophores, and structural motifs. The structures displayed in Charts 1–4 are selected and surveyed before discussion of their photophysical properties.

Mono-Platinum Acetylide Chromophores. A benchmark in platinum acetylide chemistry and photophysics is bis-((4-(phenylethynyl)phenyl)ethynyl)bis-(tributylphosphine)platinum(II), commonly abbreviated as **PE1** (**1**, Chart 1). As shown in Chart 1,

several series based on **PE2** have been synthesized, including platinum acetylides with varying numbers of phenylene-ethynylene repeat units (**1–3**);⁹ chloroplatinum complexes with one ligand mimicking half of **PE2** (**4–6**);⁴⁹ platinum phenylene-ethynylenes with sydnones on the peripheral phenyl rings (**7–9**);⁵⁰ and asymmetric platinum phenylene-ethynylene complexes where the conjugation lengths are different on either side (**10–12**).⁵¹ Substitution of one phenylene ring with 2-thienyl and 2,5-thienylene in **PE2** (**13–14**) has been reported by Glimsdal in 2007.¹⁰ Platinum acetylides end-functionalized with multiple generations of the 2,2-bis(methylol)propionic acid (bis-MPA) dendron, **15–17**, were reported by Malmström and co-workers in 2006.⁵² A divergent approach was adapted to

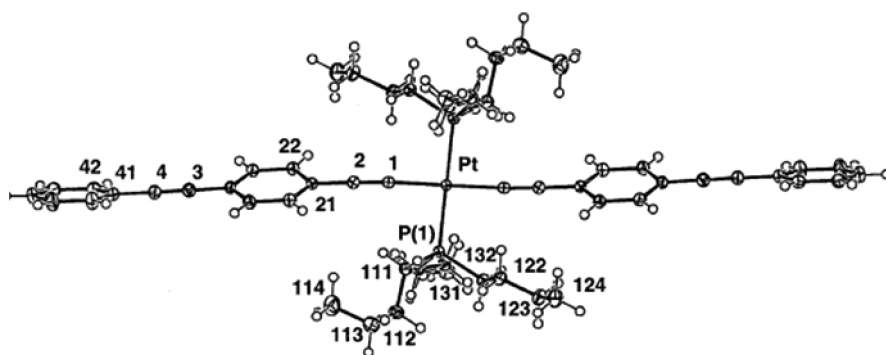


Figure 4. ORTEP diagram of PE2, with thermal ellipsoids drawn at 50% probability level. Reprinted with permission from ref 53. Copyright 2002 John Wiley & Sons.

synthesize the arylalkynyl end-functionalized with bis-MPA utilizing the versatile chemistry of acetonide protected bis-MPA anhydride, and the arylalkynyl dendrons were coupled with *trans*-Pt(PBu₃)₂Cl₂ via Hagihara coupling.

To illustrate important structural features of the monoplatinum complexes, we show the crystal structure of PE2⁵³ in Figure 4. The molecule has a slightly distorted square planar geometry, with a P(1)–Pt–C(1) angle of 86.6°, consistent with the Pt(II) d⁸ configuration. The bond lengths of Pt–P(1) and Pt–C(1) are 2.308 and 1.996 Å, respectively. The phenyl rings are twisted out of the plane defined by P2PtC2; this is consistent with DFT calculations that indicate the “twisted” conformation is slightly more stable than the all planar geometry.^{54,55}

In 2007, Rogers and co-workers reported the photophysical characterization of a series of fluorenyl-derivatized platinum acetylides that incorporate 2PA chromophores in a D–π–D or A–π–A motif (structures 18–21).²⁸ These complexes incorporate either a benzothiazole-2,7-fluorenyl (FB, 18) or a diphenylamino-2,7-fluorenyl (DPAF, 19) ligand. Originally developed at the Air Force Research Laboratory, the FB and DPAF ligands are 2PA chromophores that have high two-photon absorption cross sections (σ_2) and they possess electron-donating (DPAF) or electron-withdrawing (FB) character. The linear and nonlinear photophysical properties of these highly efficient 2PA platinum acetylide chromophores is discussed further below.

Di-Platinum Acetylide Chromophores. In 2001, Köhler and co-workers reported several diplatinum acetylides (22–29), featuring long conjugated chromophores and strong electron donors or acceptors incorporated into the ligands.⁵⁶ Their work on these diplatinum acetylides provides insight into the excited-state structure and electronic delocalization of the corresponding Pt-acetylide based π-conjugated polymers. In 2010, we reported diplatinum acetylides with the general structure DPAF–C≡C–Pt(PBu₃)₂–C≡C–Ar–C≡C–Pt(PBu₃)₂–DPAF as shown in Chart 3. The central arylene core is systematically varied with increasing electron-withdrawing ability, including 1,4-phenylene (30), 2,5-thienylene (31), 5,5′-(2,2′-bithienylene) (32), 2,5-(3,4-ethynylene dioxy)thienylene (33), 2,1,3-benzothiadiazole (34), and 4,7-dithien-2-yl-2,1,3-benzothiazole (35).²⁷

Platinum Polyene Structures. Platinum polyenes are of interest because of their applications in photovoltaic solar cells and light-emitting devices.^{4,31,57–61} Since the photophysical studies of polymers can be complicated because of the polydispersity and chain defects in the backbone, well-defined conjugated oligomers with multiple platinum metal centers are often studied.⁵⁴ For example, experimental and theoretical investigations

on platinum acetylide oligomers and polymers have explored the relationship between structure and the delocalization of the singlet and triplet excitons and how the excitons migrate.⁴⁶ For 36, (Chart 4), the ground-state absorption and fluorescence of the platinum acetylide oligomers indicate that the singlet excited state is delocalized over several repeat units.³⁴ The phosphorescence is less affected by conjugation length, signifying a more localized triplet excited state (concentrated on one or two units of [–Pt(PBu₃)₂–C≡C–Ph–C≡C–]). For 37 (Chart 4), quantum chemical calculations, in addition to the absorption, emission, and excited-state absorption, give evidence that the lowest triplet excited state, T₁, is localized on one phenylene ring within the polymer system.⁵⁴ The conformation of the phenylene repeat unit (planar versus perpendicular with respect to the Pt(PBu₃)₂ plane), directly influences the absorption and phosphorescence energies.⁵⁵

In 2010, Wong, Harvey and co-workers reported a platinum polyene with 1,3,4-oxadiazole and fluorene units.⁶² X-ray crystallography of the corresponding oligomer of the polyene confirms the unique planarity, which is essential for good π-conjugation across the chain. The oxadiazole unit has high electron affinity and good electron-transporting properties, which renders it useful in polymer light-emitting devices (PLED). Incorporation of fluorene units into the polymer chain enhance the two-photon cross-section compared to the nonfluorene substituted oxadiazole polymer. The results suggest that the hybrid structure of electron-rich fluorene and electron-poor oxadiazole provide efficient building units for 2PA materials.

LINEAR OPTICAL PROPERTIES

Platinum acetylide chromophores typically display ground state absorption in the UV region ($\lambda < 420$ nm) and they are relatively transparent throughout the visible region. Nevertheless, by incorporating segments of alternating donor–acceptor arylene units, low band gap platinum acetylide polymers can be obtained featuring strong absorption in the visible region for application in photovoltaic solar cells.^{4,57,60,61} The incorporation of the platinum metal into the conjugated organic framework induces phosphorescence, typically between 500–650 nm, whereas fluorescence is characteristically exhibited near the ground state absorption bands (in the blue or violet region) with a relatively small Stokes shift. Though phosphorescence of some platinum acetylide complexes can only be observed at low temperature, many systems exhibit strong phosphorescence at room temperature, suggesting that the rate of ISC between the

Chart 2. Platinum Acetylide Chromophores with High Two-Photon Absorption Cross-Section

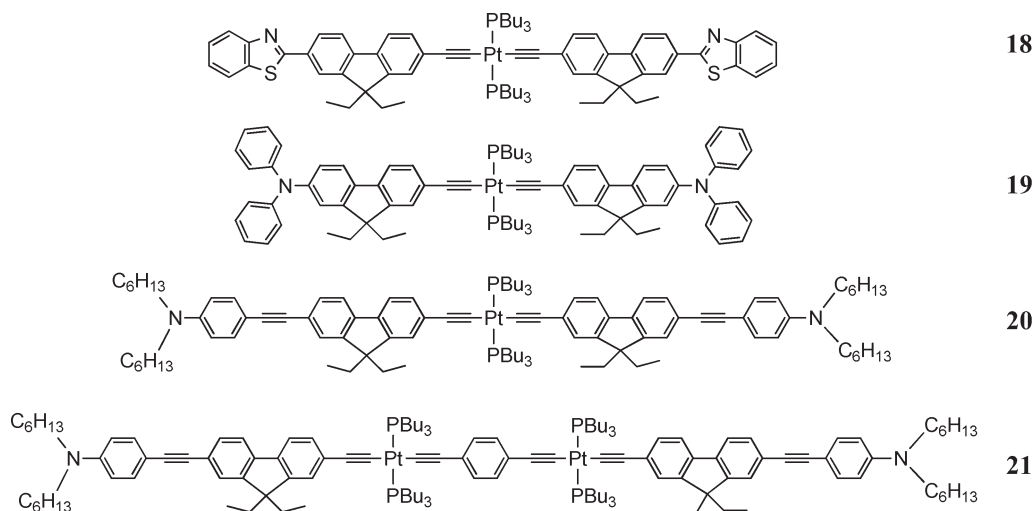


Chart 3. Di-platinum Acetylide Chromophores

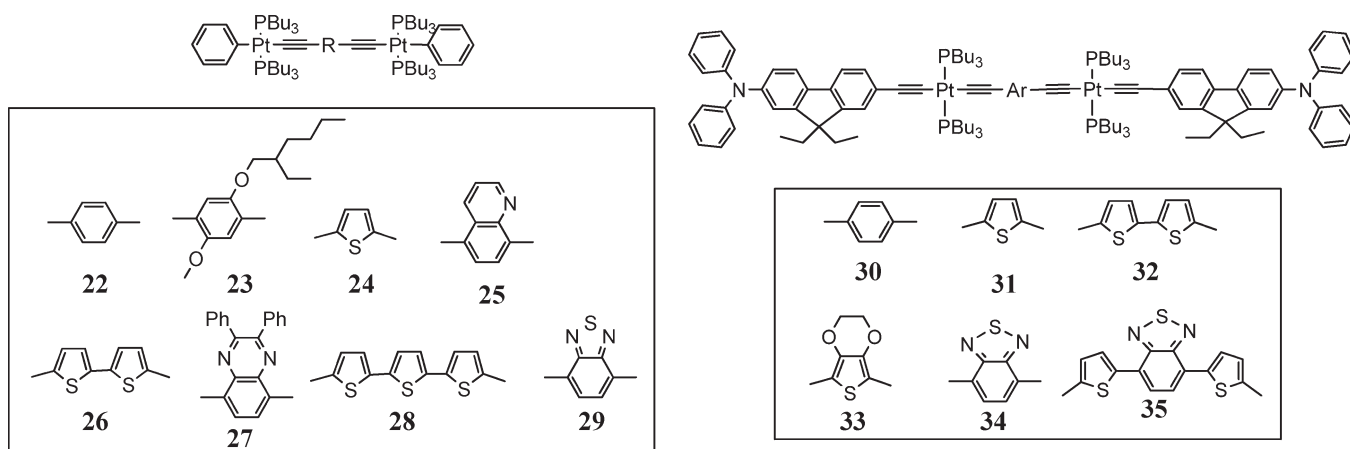
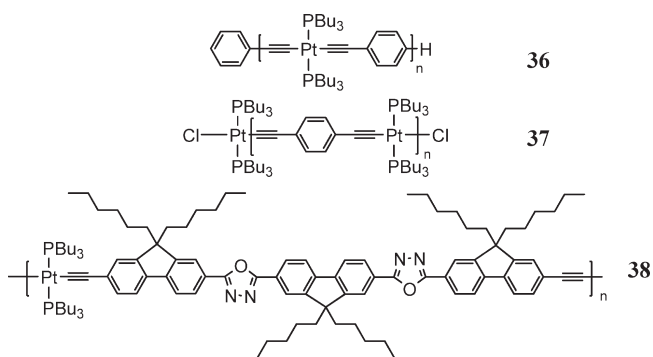


Chart 4. Platinum Acetylide Oligomers and Polymers



singlet and triplet manifolds is efficient. The triplet excited state of platinum acetylide chromophores has a lifetime in the micro-second time domain, and it typically exhibits broad and strong T_1 – T_n absorption in the visible and near-infrared regions. To

illustrate some of the important features of the linear photophysical properties characteristic of platinum acetylide chromophores, the ground state absorption, photoluminescence, and triplet–triplet absorption-difference spectra of **18**–**21** are shown in Figure 5.²⁸

Variation in conjugation length, ligand choice, and overall complex design lead to changes in the absorption and emission spectra, allowing for systematic modification and tuning of the photophysical properties of platinum acetylide chromophores. The linear photophysical properties of several representative platinum acetylide chromophores are listed in Table 1.

In 2002, Cooper and co-workers reported the effect of conjugation in the PE_n series (**1**–**3**, Table 1).⁹ Conjugation through the platinum center occurs in the singlet state, as demonstrated by the observed red-shift of the absorption and fluorescence of **1**–**3** compared with the corresponding butadiynes that lack the Pt(II) center, $(Ph-C\equiv C)_n-(C\equiv C-Ph)_n$.⁶³ The $S_0 \rightarrow S_1$ absorption of **1** is attributed to metal-to-ligand charge transfer (MLCT). In addition to the MLCT character, the absorption of **2** and **3** are unique with increasing

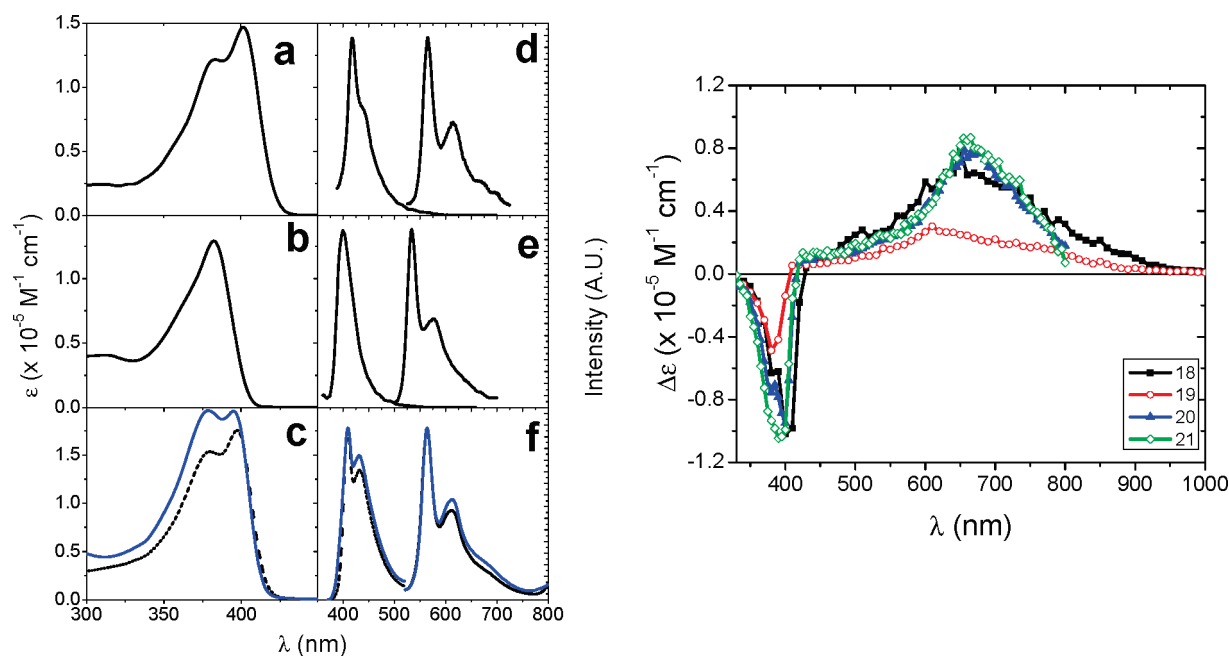


Figure 5. Left panel: ground-state absorption of (a) **18**, (b) **19**, (c) **20** (dashed line), and **21** (blue solid line) in air-saturated benzene solutions; right panel, photoluminescence spectra in deoxygenated benzene solution of compound (d) **18**, (e) **19**, (f) **20** (dashed line), and **21** (blue solid line). Right Panel: Transient absorption difference spectra of **18–21** in deoxygenated benzene solutions following excitation at 355 nm. Reprinted with permission from ref 28. Copyright 2007 American Chemical Society.

$\pi-\pi^*$ character due to the increased conjugation in the aryl acetylide ligands. The phosphorescence of **1–3** is blue-shifted compared to $(\text{Ph}-\text{C}\equiv\text{C})_n-(\text{C}\equiv\text{C}-\text{Ph})_m$, suggesting that the lowest triplet excited state T_1 is most likely confined to a single phenylene ethynylene ligand. The introduction of the platinum center has the following effects on spectral and kinetic photophysical properties as demonstrated by the properties of **1–3**:⁶³ (1) there is conjugation through the platinum center, but the triplet excited state T_1 is confined to a single ligand; (2) compared with the free phenylene ethynylene ligand, in the corresponding platinum complexes the fluorescence quantum yield (Φ_f) is lower and the quantum yield for ISC (Φ_{ISC}) is larger because of the spin–orbit coupling induced by the metal; (3) the triplet lifetime is less compared to the free butadiyne ligand; (4) the effects of the platinum center are largest in the small complex (**1**), and the influence of metal decreases as ligand size increases.

Cooper and co-workers also investigated the localization of singlet and triplet excited states in the unsymmetrical mono-platinum acetylide complexes (**10–12**, Table 1) with the molecular formula $L_1-\text{Pt}-L_2$, where L_1 and L_2 are different π -conjugated phenylene ethynylene ligands.⁵¹ Density functional calculations were applied to compute the geometry and energy of the ground singlet and lowest triplet (T_1) states. The combination of the computational results with the observed spectroscopic properties provided evidence that the singlet excited state is delocalized through the metal center, whereas the triplet is confined to the lowest energy, and largest, aryl acetylide ligand.

The linear optical properties of the fluorenyl-derivatized platinum acetylides (**18–21**, Chart 2) are largely determined by their ligands,²⁸ such as benzothiazole-2,7-fluorene (FB, **18**) and diphenylamino-2,7-fluorene (DPAF, **19**). For example, compounds **18** and **19** exhibit room temperature phosphorescence, with phosphorescence maximum at $\lambda_{\text{ph}} \approx 565$ and 534 nm (Table 1 and Figure 5), respectively. The phosphorescence of **18**

has a longer wavelength maximum, consistent with extended π -conjugation in the FB ligand. Photophysical studies also demonstrate that the singlet excited state is delocalized across the Pt center to the two conjugated ligands, while the triplet exciton is localized on a single conjugated ligand. As illustrated in Figure 5, the triplet excited states of **18–21** are characterized with large triplet–triplet absorptivity ($\epsilon_{\text{TT}} > 5 \times 10^{-4} \text{ M}^{-1} \text{ cm}^{-1}$) and long lifetime ($>100 \mu\text{s}$), indicating efficient excited state absorption in these systems. The complexes **18–21** also exhibit large 2PA cross-sections as discussed in the next section.

The unique photophysical features of **30–35** (Chart 3) lie in the triplet excited states which are shown to be concentrated on the central unit of $-\text{Pt}(\text{PBu}_3)_2-\text{C}\equiv\text{C}-\text{Ar}-\text{C}\equiv\text{C}-\text{Pt}(\text{PBu}_3)_2$.²⁷ The triplet energy can be determined by phosphorescence (λ_{ph}) and varies in the order of **30** > **31** > **33** > **32** (Table 1). Phosphorescence from **34** and **35** was not observed in the visible region, but given that the absorption spectra of these two complexes are significantly red-shifted, their triplet energy is considered to be lower than **32** and likely the phosphorescence occurs in the near-infrared region. The triplet–triplet absorption of **30–35** exhibits strong and broad absorption in the visible region 600–800 nm.

In addition to the experimental investigations described above, a theoretical study of the 1PA processes of the platinum acetylide species with 2PA chromophores was carried out by Yang et al. in 2008.⁶⁴ Optimizations of the ground state geometry of the examined platinum acetylide species show that the alkynyl-fluorene/benzene plane is almost perpendicular to the plane defined by the PtL_2C_2 unit. Additionally, the calculations suggest that the HOMO consists mainly of ligand based π -orbitals mixed with $d\pi$ orbitals of the platinum center, whereas the LUMO is mainly antibonding π^* orbitals in the aryl acetylide ligands without any contribution from the metal center. As such, the HOMO/LUMO transition is primarily $\pi-\pi^*$ transition with a small fraction of MLCT character.

Table 1. 1PA Photophysical Properties

compound	solvent	λ_{\max} (nm)	ϵ ($\times 10^4$ M $^{-1}$ cm $^{-1}$)	λ_{fl} (nm)	λ_{ph} (nm)	T_1-T_n (nm)	τ (μ s)	ref
1	benzene	324	2.5	364	498	^a	590 \pm 150 ps	9,63
2	benzene	355	8.9	385	527	575	42	9,63
3	benzene	377	8.5	400	557	630	86	9,63
10	benzene	349	5.8	377	590	590	93	51
11	benzene	357	6.9	403	650	650	144	51
12	benzene	359	10	401	650	650	160	51
18	THF	402	15	418	565	670	126	28
19	THF	383	13	399	534	610	117	28
30	THF	382	17	401	537	627	40	27
31	THF	386	18	414	607	623	10	27
32	THF	381	11	459	729	634	4.5	27
33	THF	387	13	433	637	567	4.6	27
		407	12					
34	THF	375	15	584	^b	700	^b	27
		490	3.6					
35	THF	380	19	698	^b	679	^b	27
		551						

^a Unable to determine because of the short lifetime of the triplet state. ^b Phosphorescence is expected in the near-infrared region.

NONLINEAR ABSORPTION PROPERTIES

Data Collection and Techniques. The propensity of a chromophore to exhibit nonlinear absorption of ultrashort (fs) pulses is related to the chromophore's two-photon cross-section (σ_2) the value of which is typically listed in units of Goeppert-Mayer (GM, 1 GM = 1×10^{-50} cm 4 s photon $^{-1}$). When measurements are carried out with pulses of longer duration (ps or ns) an effective 2PA cross section is measured (σ_2') which also includes contributions from singlet–singlet and/or triplet–triplet excited state absorption; thus, σ_2' is typically much larger than the intrinsic 2PA response as quantified by σ_2 . The σ_2' is dependent upon the pulse width and the pulse repetition frequencies (prf). To measure σ_2 with the greatest accuracy, lower prf is desirable. The cross-sections can be determined by two major techniques, the nonlinear transmission method (NLT), and luminescence measurement (i.e., two-photon excited fluorescence, 2PEF).

The NLT method measures the nonlinear transmission as a function of the light intensity. A common NLT technique is the “Z-scan” which fixes the input energy of a focused laser beam while changing the distance between the sample and the laser focal plane.⁶⁵ The Z-scan measures the nonlinear refractive index and nonlinear absorption coefficient of a sample, as described elsewhere.^{65,66} As illustrated in Figure 6, the closed-aperture Z-scan can measure both nonlinear refractive index and nonlinear absorption coefficient by employing an aperture in the far field that allows only the light in the central area to reach the detector. The open-aperture Z-scan technique removes the aperture collecting all of the transmitted light, providing the ability to measure only the nonlinear absorption coefficient of a material. To determine a chromophore's σ_2 by Z-scan, we need to measure both the local intensity I_0 and the nonlinear transmission. The local intensity I_0 is related to the energy and time duration of the incident laser pulse, as well as the diameter of the beam focus (the “waist”), the latter of which is difficult to determine due to effects such as self-focusing and self-defocusing. Ever after careful elimination of the possible interferences in

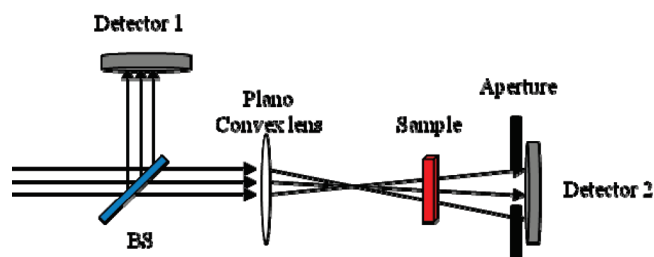


Figure 6. Schematic diagram of a simple closed-aperture Z-scan apparatus.

measurement of I_0 , σ_2 values determined by Z-scan will typically have 10–20% error.

Examples of nonlinear transmission and Z-scan data for platinum acetylide complexes are shown in Figure 7. As can be seen in Figure 7a, the diplatinum acetylides **30–33** show remarkable nonlinear response for laser with nanosecond pulse width at 600 nm and a clamping energy of ~ 100 μ J.²⁷ The nonlinear strength varies in the order of **30** < **31** \approx **33** < **32**. Z-scan data with excitation with a nanosecond laser for complexes **PE2**, **18** and **19** is shown in Figure 7b, and the effective NLA strength increases in the order of **PE2** < **18** < **19**.⁶⁷ As will be discussed further, efficient σ_2 , large triplet–triplet cross-section (σ_{T-T}), and large Φ_{ISC} can enhance the effective NLA strength with respect to nanosecond pulses.

To avoid using high-power and high-energy pulsed lasers that are typically required by the NLT method, the alternative method of relative fluorescence (2PEF) measurements can be employed to determine σ_2 . This method compares the two-photon induced luminescence intensity of a new compound to a known reference, and in principle it corrects for the temporal and spectral beam profile variations of the excitation pulse.^{68,69} Intrinsically, σ_2 obtained by 2PEF is twice that obtained with NLT techniques based on definition.^{70,71} For the sake of comparison, all the σ_2 values reported herein are corrected to be relative to measurements done by NLT. In a 2PEF measurement, it is

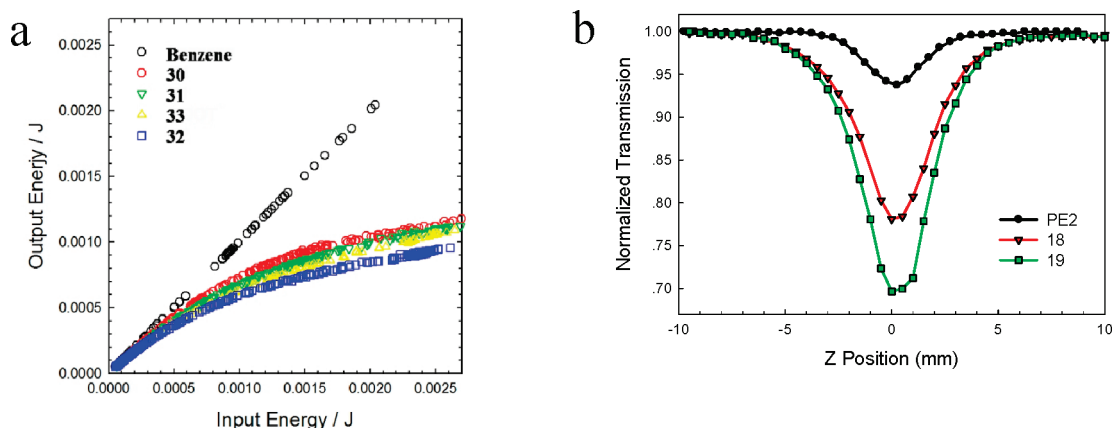


Figure 7. (a). Nonlinear transmission of diplatinum complexes **30–33** in benzene solutions ($c = 20$ mM). Laser pulses from Nd/YAG pumped OPO tuned to 600 nm (pulse width ~ 10 ns). Reprinted with permission from ref 27. Copyright 2010 American Chemical Society. (b) Nanosecond open aperture Z-scan response of **PE2**, **18**, and **19** in THF ($c = 1$ mM), 600 nm excitation from Nd:YAG pumped OPO, ~ 750 μ J/pulse, (pulse width ~ 10 ns).⁶⁷

Table 2. Intrinsic 2PA Cross-Section Values (σ_2) for PE2 and Its Derivatives

complex	method	solvent	excitation wavelength (nm)	σ_2 (GM)	pulse repetition frequency	ref
PE2	Z-scan, fs	THF	720	7	4.5 MHz	52
13	Z-scan, fs	THF	740	7.1	9 kHz	10
			740	17	1 MHz	
14	Z-scan, fs	THF	740	5.5	9 kHz	10
			740	9.5	1 MHz	
15	Z-scan, fs	THF	740	8.9	9 kHz	52
			740	15	1 MHz	
16	Z-scan, fs	THF	740	~ 10	^a	52
			740	16	4.75 MHz	
17	Z-scan, fs	THF	740	~ 10	^a	52
			740	215	4.75 MHz	

^a Measured at the low frequency limit between 9–100 kHz.⁵²

typically assumed that the 2PA-induced fluorescence quantum yield (Φ_{2PA}) is the same as that under 1PA-excitation (Φ_f). Commercial organic reference dyes with fluorescence emission spanning 375–900 nm and 2PA spanning 550–1600 nm have been examined to provide visible and near-infrared references.⁶⁸

Benchmark Complexes: PE2 and Derivatives. The simple symmetrical phenylene-ethynylene substituted platinum acetylide complex, **PE2**, has served as a benchmark for optical power limiting (OPL) studies since McKay and co-workers first reported its nonlinear optical properties in 1998.²⁴ **PE2** exhibits enhanced 2PA/RSA in the visible and near-infrared regions due to its unit intersystem crossing yield to the triplet manifold and strong triplet–triplet absorption.⁴⁶ Additionally, the triplet excited state absorption cross-section is independent of the singlet excitation pathway.⁷² The 2PA coefficient (β) of **PE2** was reported as 0.34 cm/GW at 595 nm, which corresponds to 235 GM at 595 nm. This measurement was carried out using picosecond laser pulses (27 ps), and it is likely that the measured value includes significant ESA contributions from both the singlet and triplet excited states in addition to pure 2PA.^{25,73} Recently, Glmsdal and co-workers measured the intrinsic σ_2 of **PE2** to be 7 GM at 720 nm using Z-scan method with femtosecond pulses (180 fs).^{10,74}

Besides **PE2**, a variety of **PE2** derived platinum acetylides have been studied as nonlinear absorbing materials,^{10,52,75,76} and their 2PA cross-section values are listed in Table 2. As the typical experimental uncertainty of σ_2 measurement is 10–20%, we only report the two significant digits of the values and neglect the errors.

The NLA properties of the (thienylene phenylene) derivatives **13** and **14** (Chart 1) were examined relative to **PE2** by Glmsdal and co-workers in 2007.^{10,75} These (thienylene phenylene) Pt acetylides incorporate thiophene as the “interior” arylene unit or on the “periphery” of the oligomer. The intrinsic 2PA cross sections σ_2 of **13** and **14** were measured by Z-scan with 180 fs Ti/Sapphire laser excitation at 740 nm and are listed in Table 2. Note that during the measurement, a pulse picker was used to regulate the laser with pulse repetition frequency (prf) between 9 kHz and 4.75 MHz. The σ_2 values from higher repetition frequency are larger, which is likely due to a contribution from excited state absorption. For example, the σ_2 values obtained with 9 kHz prf are 7.5 GM and 5.5 GM for **13** and **14**, respectively. When the frequency was turned to 1 MHz, σ_2 values are 17 GM and 9 GM for **13** and **14**, apparently due to the excited state absorption. From a practical point of view, an important parameter that is relevant for OPL applications is the clamping level, above which the output energy is approximately constant as a function of

input energy. The clamping level at 532 nm is 5.0 and 7.6 μJ for 13 and 14, respectively (E_{in} is 150 μJ).⁷⁵

In 2006, Malmström and co-workers reported the NLA properties of dendritic PE2 derivatives (15–17, Chart 1).⁵² Polyester dendrons up to the fourth generation were grown divergently and incorporate the PE2 chromophore, which was discussed above.⁵² The highly branched, well-defined structures with a large number of modifiable end groups lead to encapsulation of the PE2 chromophore into the inner part of the dendritic structure, as well as controlling solubility, hydrophobicity, and the ability to cross-link the materials in a film. The intrinsic σ_2 of the dendron-encapsulated chromophores were determined to be ~ 10 GM at low prf (less than 100 kHz) using the femtosecond Z-scan method at 720 nm. However, with a higher prf of 4.75 MHz, the “effective” 2PA cross-section for PE2, 16, and 17 is 7, 16, and 215 GM, respectively. As illustrated in Figure 5, the high pulse repetition frequency of 4.75 MHz allows the population of the long-lived triplet excited state to accumulate, resulting in a dramatic increase of the Z-scan response for the higher generation 17. The dendron-decorated 16 and 17 display more efficient shielding of the dye moiety resulting in a decrease of the triplet–triplet annihilation recombination rate, leading to a much stronger Z-scan signal.⁵² On the other hand, the

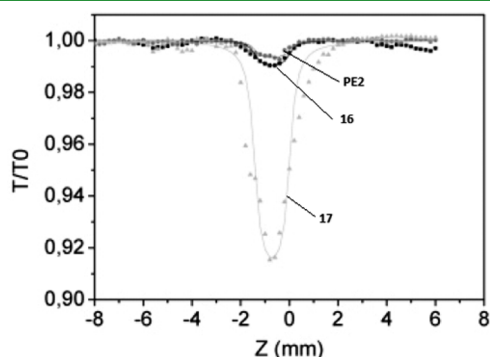


Figure 8. Z-scan of PE2, 16, and 17 using the output of a femtosecond laser at 720 nm and 4.75 MHz pulse repetition frequency. Reprinted with permission from ref 52. Copyright 2006 American Chemical Society.

Z-scan of PE2 is weak (Figure 8), indicating fast quenching in the PE2 triplet state. The OPL properties of the complexes were measured with 30 mM THF solutions at three different wavelengths: 532, 580, and 630 nm. A general trend is that the higher generation of the dendron, the lower the clamping level. For example, the clamping level at 532 nm is 9, 7.6, 6.3, and 6.6 μJ for PE2, 15, 16, and 17, respectively, with all the dendron-decorated platinum acetylide showing superior OPL performance than PE2. The large dendrons are believed to prevent oxygen quenching as well as prevent aggregation of the dyes, and therefore increase the OPL responses of the chromophores.

Benchmark Complexes: Other Platinum Acetylides. Researchers have also explored the NLA properties of platinum acetylides that are structurally distinct from PE2, including (1) modification of the alkynyl ligand with highly π -conjugated fluorenyl chromophores, as seen in 18–21 (Chart 2);²⁸ (2) dimeric platinum complexes with the general structure $\text{DPAF}-\text{C}\equiv\text{C}-\text{Pt}(\text{PBu}_3)_2-\text{C}\equiv\text{C}-\text{Ar}-\text{C}\equiv\text{C}-\text{Pt}(\text{PBu}_3)_2-\text{C}\equiv\text{C}-\text{DPAF}$, where Ar is an arylene group and DPAF is a strong π -conjugated donor, as seen in 30–35 (Chart 3);²⁷ (3) branched platinum acetylides with conjugated cores such as oxadiazole and truxene, as seen in 39–44 (Chart 5).⁷⁷ The 2PA cross-section values of these platinum acetylides are listed in Table 3.

In 18–21, the simple phenylene-ethynylene ligand in PE2 is replaced with a strong π -conjugated donor and acceptor, and the resulting D– π –D and A– π –A complexes show enhanced NLA in the near-infrared region.²⁸ The 2PA cross-sections of 18–21 have been reported to vary between 60–370 GM (Table 3) at 720 nm using 2PEF method with femtosecond pulsed laser excitation. The 1P- and 2PA spectra of 18–21 are similar, and the spectrum of 18 is shown in Figure 9 as a representative example. The 2PA spectra are characterized with two bands, one coinciding with the corresponding 1PA peak at $\lambda_{\text{ex}} \approx 2\lambda_{1\text{PA}}$, while the other considerably blue-shifted relative to $2\lambda_{1\text{PA}}$. The observation of a strong band in the 2PA spectrum between 750 and 850 nm, which overlaps with $2\lambda_{1\text{PA}}$ is in conflict with the usual selection rules for centrosymmetric chromophores, which indicate that the transition to the lowest excited state is forbidden in 2PA. The explanation is that in solution there are at least two conformers for the platinum acetylides, and the

Chart 5. Branched Platinum Acetylide Oligomers

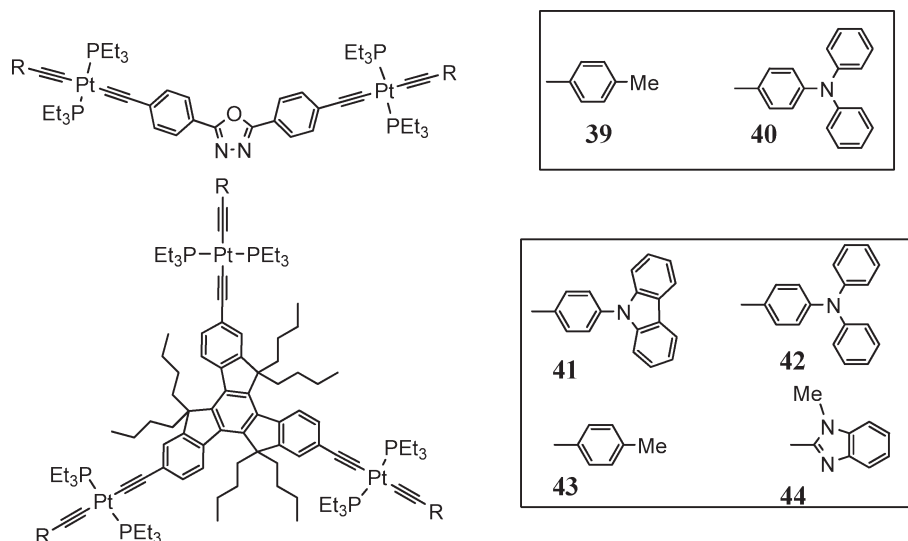


Table 3. Intrinsic 2PA Cross-Section Values (σ_2) for Platinum Acetylides other than PE2

compd	method	solvent	excitation wavelength (nm)	σ_2 (GM)	pulse repetition frequency (kHz)	ref
18	2PEF, fs	benzene	720	370	1	28
19	2PEF, fs	benzene	720	140	1	28
20	2PEF, fs	benzene	720	60	1	28
21	2PEF, fs	benzene	720	160	1	28
30	2PEF, fs	THF	724	88	1	27
31	2PEF, fs	Toluene	732	260	1	27
32	2PEF, fs	Toluene	734	200	1	27
33	2PEF, fs	Toluene	730	190	1	27
34	2PEF, fs	THF	756	230	1	27
35	2PEF, fs	THF	760	230	1	27
39	2PEF, fs	benzene	720	17	1	77
40	2PEF, fs	benzene	720	41	1	77
41	2PEF, fs	benzene	720	21	1	77
42	2PEF, fs	benzene	720	32	1	77
43	2PEF, fs	benzene	720	27	1	77
44	2PEF, fs	benzene	720	11	1	77

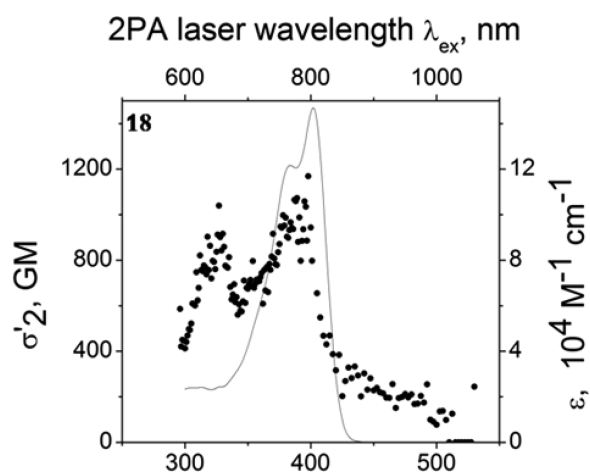
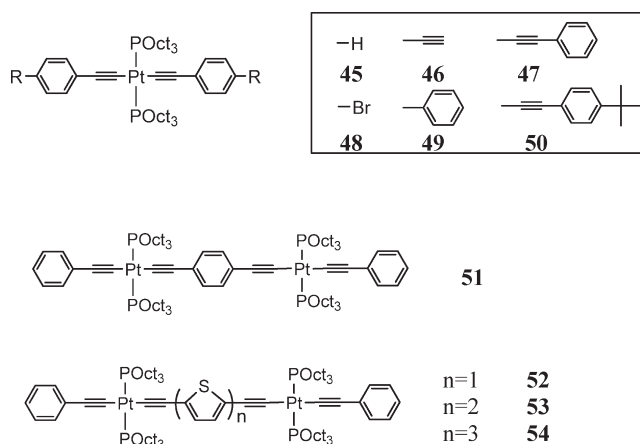


Figure 9. Two-photon absorption spectrum of **18** dissolved in benzene at ambient conditions. The cross-section σ_2 was measured by 2PEF using femtosecond laser pulses. Note that this σ_2 is twice that obtained by NLT. One-photon absorption (solid line) is shown for comparison. Reprinted with permission from ref 28. Copyright 2007 American Chemical Society.

2PA transition which is observed at $2\lambda_{1PA}$ arises from the noncentrosymmetric conformer. The blue-shifted band between 600–700 nm comes from the two-photon allowed gerade–gerade transition, which reflects the inversion symmetry as well as the involvement of the Pt atom in the molecule.

Another approach to improve OPL properties of platinum acetylides is to create chromophores that simultaneously show efficient σ_2 , large Φ_{ISC} , and large triplet–triplet cross-section (σ_{T-T}). Utilizing the efficient 2PA chromophore DPAF,²⁸ the 2PA transitions of compounds **30–35** (Chart 3) originate from the DPAF chromophore and span the region of 600–1000 nm, with σ_2 (88–260 GM in Table 2), approximately two times larger than that of the DPAF unit alone (44 GM at 740 nm). Despite the fact that the arylene cores have different electron-withdrawing ability, the maximum σ_2 values of **30**, **31**, **32**, and **33** are similar, indicating “shielding effect” on the dipole moment by the platinum center toward the arylene core. Moreover, the triplet–triplet transient

Chart 6. Liquid Platinum Acetylide Oligomers



absorption spectra overlap with 2PA in 600–800 nm, enhancing the overall NLA toward nanosecond laser pulses.

Yam, Cheah and co-workers investigated the branched platinum acetylides with oxadiazole and truxene as cores (**39–44**, Chart 5).⁷⁷ These molecules are constructed with oxadiazole and truxene as cores and various electron-donating groups, such as the triphenylamine and carbazole as the peripheral units. The cores are unique because of their rigid and planar structure, good thermal and chemical stability, and rich photophysical properties such as high luminescence quantum yield. The 2PA values are reported in the 11–41 GM range (Table 2), which are larger than **PE2**, but smaller than the fluorenyl-substituted platinum acetylides. The σ_2 values are measured by 2PEF in C_6H_6 using fluorescein in methanol (19 GM) as actinometer, with excitation provided by a mode-locked femtosecond Ti:Sapphire laser (120 fs pulse widths, 1 kHz repetition rate) at 720 nm.⁷⁸

PLATINUM ACETYLIDE MATERIALS

Liquids. **PE2** and its derivatives have only moderate solubility in organic solvents,²⁴ and the parent molecule is not suitable for

photophysical studies such as exciton migration and triplet–triplet annihilation (TTA), which require concentrated solutions in order to produce a high concentration of excited states. In 2004, Cooper and co-workers reported the synthesis and characterization of a series of PE2 derived liquid platinum acetylides (**45–50**, Chart 6) at ambient temperature.⁷⁹ The liquid state of these complexes at room temperature comes from the replacement of the tributylphosphine ligands with the longer, bulkier, and more flexible trioctylphosphine ligands, which increase the entropy of the molecules and reduce the melting points below room temperature. An advantage of the liquid material is that a 10-fold increase in chromophore concentration is possible in solutions of the liquid oligomers compared to that of the saturated solutions of PE2. Not surprisingly, the triplet excited-state properties of **45–50** are the same as those of their counterparts with tributylphosphine ligands in solutions. In contrast, the triplet excited states of the neat liquid of the **45–50** show a longer lifetime (1.2 μ s) than compared to the air-saturated dilute solution of PE2 (240 ns) because of the higher viscosity of the liquid oligomers.

To further tune the absorption spectra of the platinum acetylides, another series of Pt(POct₃)₂-derived liquid platinum acetylide oligomers (**51–54**, Chart 6) was developed in our group.⁸⁰ As shown in Figure 10, the oligomers **51–54** are liquids at ambient temperature, and differential scanning calorimetry (carried out by Dr. Thomas Cooper at the Air Force Research

Lab) shows that the oligomers exhibit glass-transition temperatures in the range -60 to -73 °C. The center segment of the oligomers is varied systematically from phenyl to mono-, di-, and terthiophene, with the color of these liquids changes systematically from yellow to orange, consistent with the red-shift observed in ground state absorption due to increased π -conjugation. The triplet–triplet transient absorption spectra show broad and strong peaks in the visible and near-infrared region, with a continuous red-shift observed in the oligothiophene series ($\lambda_{T-T(\text{MAX})}$ is 600, 630, and 650 nm for **52**, **53**, and **54**, respectively). On the basis of these observations, it is possible to shift the T₁–T_n absorption even more to the near-infrared region with even longer conjugated chromophores.

Acrylate Polymers. Poly(methyl methacrylate) (PMMA) is widely used as an organic glass because of its ease of processing, good optical transparency, low density and high impact resistance. PMMA materials embedded with platinum acetylide chromophores are particularly good for OPL materials because they can be easily cut and polished for optical applications. In 2008, Malmström and co-workers successfully prepared two types of materials using PMMA as matrices for platinum acetylide chromophores:³ (1) a guest–host material obtained by physically mixing the methacrylate end group-functionalized platinum acetylide (**15**, Chart 1) with PMMA; (2) a covalently bonded material by copolymerization of a PE2 dye (**55**, Chart 7) with methyl methacrylate (MMA). The bis-MPA groups present in **55** provide good compatibility between the guest and host and prevent the π -stacking of the chromophores and also improve the solubility of the chromophores in MMA. As such, a doping level of 13 wt % of the chromophore in the host polymer was achieved. With respect to their performance as OPL materials, the guest–host materials display relative low thermal stability (T_g less than 105 °C), yet they show superior NLA properties with a lower clamping energy (less than 4 μ J for input laser energy up to 110 μ J) than the covalently bound materials (8 μ J for input laser energy up to 100 μ J).

Sol–Gel Glasses. Compared with organic glassy materials, inorganic glasses exhibit excellent optical quality, as well as increased thermal stability and higher damage threshold. In 2009, Parola, Eliasson and co-workers reported a modified sol–gel process as an efficient way to prepare platinum acetylide hybrid glass materials.⁸¹ A benzyl alcohol end-capped PE2 was grafted with reactive trialkoxysilane groups by nucleophilic reaction between the alcohol and isocyanate propyltriethoxysilane. The acid-catalyzed hydrolysis and condensation between the silane-functionalized chromophores (**56–57**, Chart 8) with methyltriethoxysilane at room temperature

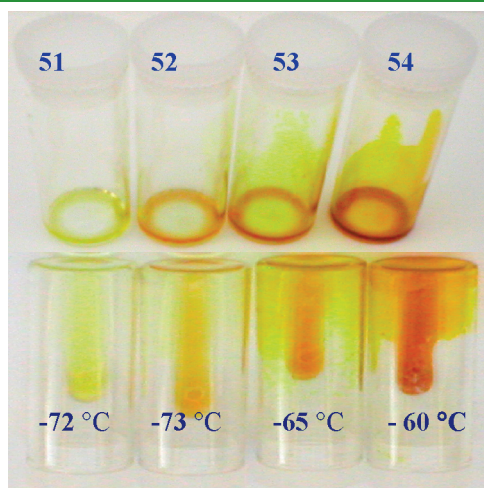


Figure 10. Vials containing liquid Pt-acetylides **51–54**. Numbers at bottom of photograph show glass-transition temperatures in °C.⁸⁰

Chart 7. PE2 End-Capped with bis-MPA/Methacrylates

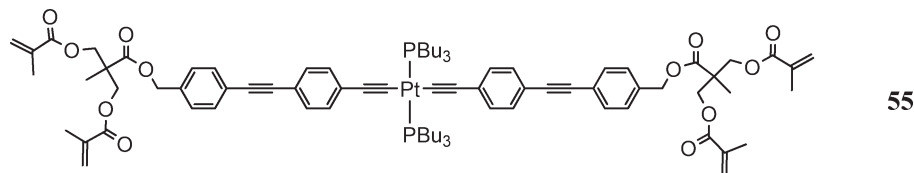
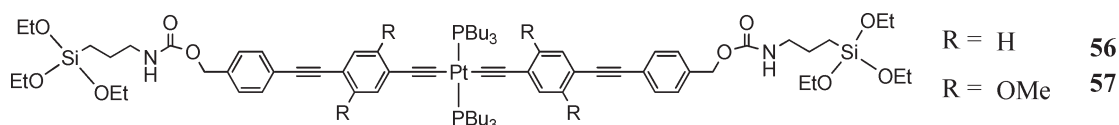


Chart 8. Chemical Structures of Silane-Functionalized Platinum Acetylide Chromophores



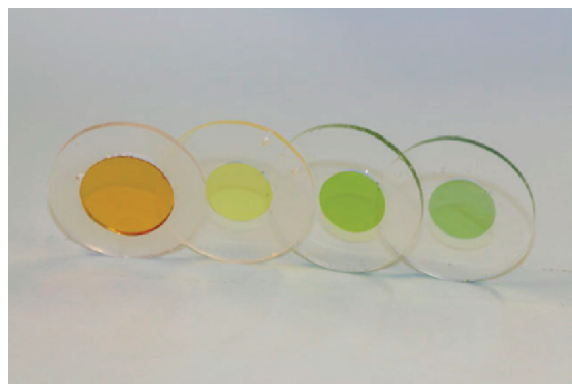


Figure 11. Examples of glass filters prepared from sol–gel hybrid monoliths and used for optical limiting applications. Reprinted with permission from ref 81. Copyright 2009 John Wiley & Sons.

generated a clear gel that could be dried from 70 to 120 °C to give the desired monoliths (Figure 11). A solid hybrid glass with 120 mM chromophore concentration has a clamping energy of 0.2, 3, 4.5, and 7 μJ at 480, 532, 580, and 630 nm, respectively with input laser energy up to 200 μJ . Recalling that dendritic PE2 derivatives have clamping values in the range of 6–8 μJ at 532 nm for 30 mM THF solutions⁵² and 30 mM thiophenyl derivatives of PE2 have clamping values between 5–8 μJ at 532 nm,⁷⁵ the NLA property of the chromophore in the sol–gel matrix is comparable to that in liquid solution or in PMMA based glasses.

SUMMARY AND CONCLUDING REMARKS

The interest in platinum acetylides as the active chromophores for OPL materials arises from the advantages of these systems compared to organic 2PA chromophores, including the ability to “mix and match” conjugated organic ligands at the Pt-center, as well as the large spin–orbit coupling provided by the metal that efficiently produces long-lived and strongly absorbing triplet excited states. In the present Spotlight Article, the synthesis and structure of a variety of platinum acetylide chromophores has been discussed. Many of these complexes are relatively straightforward to prepare via Hagihara coupling of a terminal acetylene ligand with *cis*- or *trans*-Pt(PBu₃)₂Cl₂. A number of examples are provided for the linear one-photon optical (photophysical) properties, affording the reader with a general overview of how these chromophores behave when they are illuminated with weak and moderate optical flux. More importantly, the σ_2 values and nonlinear response of state-of-art benchmark platinum acetylide chromophores are compared. Since excited state absorption plays an important role, the laser pulse duration and repetition frequency are important parameters, and these are reported as well. For practical applications, the platinum acetylide chromophores have been incorporated into liquid and solid materials such as PMMA and sol–gel hybrid inorganic glass, with the solid possessing advantages such as easy device fabrication and enhanced doping capacity. It is hoped that this Spotlight provides the reader with the perspective of how platinum acetylide chromophores and materials can serve as advanced systems for nonlinear absorption applications.

AUTHOR INFORMATION

Corresponding Author

*E-mail: kschanze@chem.ufl.edu. Tel: 352-392-9133. Fax: 352-392-2395.

ACKNOWLEDGMENT

We Air Force Office of Scientific Research (Grant AFOSR FA-9550-06-1-1084) for support. We thank Ms. Randi Price for the photograph of the PMMA glass monoliths that appears in the TOC graphic.

REFERENCES

- (1) Parthenopoulos, D. A.; Rentzepis, P. M. *Science* **1989**, *245*, 843–845.
- (2) Dvornikov, A. S.; Rentzepis, P. M. *Opt. Commun.* **1995**, *119*, 341–346.
- (3) Westlund, R.; Malmstrom, E.; Lopes, C.; Ohgren, J.; Rodgers, T.; Saito, Y.; Kawata, S.; Glimsdal, E.; Lindgren, M. *Adv. Funct. Mater.* **2008**, *18*, 1939–1948.
- (4) Guo, F.; Kim, Y.-G.; Reynolds, J. R.; Schanze, K. S. *Chem. Commun.* **2006**, 1887–1889.
- (5) Kawata, S.; Sun, H.-B.; Tanaka, T.; Takada, K. *Nature* **2001**, *412*, 697–698.
- (6) Denk, W.; Strickler, J. H.; Webb, W. W. *Science* **1990**, *248*, 73–76.
- (7) Bhawalkar, J. D.; Kumar, N. D.; Zhao, C. F.; Prasad, P. N. *J. Clin. Laser. Med. Surg.* **1997**, *15*, 201–204.
- (8) Glik, E. A.; Kinayyigit, S.; Ronayne, K. L.; Towrie, M.; Sazanovich, I. V.; Weinstein, J. A.; Castellano, F. N. *Inorg. Chem.* **2008**, *47*, 6974–6983.
- (9) Rogers, J. E.; Cooper, T. M.; Fleitz, P. A.; Glass, D. J.; McLean, D. G. *J. Phys. Chem. A* **2002**, *106*, 10108–10115.
- (10) Glimsdal, E.; Carlsson, M.; Eliasson, B.; Minaev, B.; Lindgren, M. *J. Phys. Chem. A* **2007**, *111*, 244–250.
- (11) Belfield, K. D.; Yao, S.; Bondar, M. V. In *Photoresponsive Polymers I*; Springer-Verlag: Berlin, 2008; Vol. 213, pp 97–156.
- (12) Zhou, G.-J.; Wong, W.-Y.; Lin, Z.; Ye, C. *Angew. Chem., Int. Ed.* **2006**, *45*, 6189–6193.
- (13) Zhou, G.-J.; Wong, W.-Y. *Chem. Soc. Rev.* **2011**, *40*, 2541–2566.
- (14) Rumi, M.; Barlow, S.; Wang, J.; Perry, J. W.; Marder, S. R. In *Photoresponsive Polymers I*; Springer-Verlag: Berlin, 2008; Vol. 213, pp 1–95.
- (15) He, G. S.; Tan, L.-S.; Zheng, Q.; Prasad, P. N. *Chem. Rev.* **2008**, *108*, 1245–1330.
- (16) Nguyen, K. A.; Day, P. N.; Pachter, R. *Theor. Chem. Acc.* **2008**, *120*, 167–175.
- (17) Rogers, J. E.; Slagle, J. E.; McLean, D. G.; Sutherland, R. L.; Brant, M. C.; Heinrichs, J.; Jakubiak, R.; Kannan, R.; Tan, L.-S.; Fleitz, P. A. *J. Phys. Chem. A* **2007**, *111*, 1899–1906.
- (18) Zhou, G.-J.; Wong, W.-Y.; Cui, D.; Ye, C. *Chem. Mater.* **2005**, *17*, 5209–5217.
- (19) Zhou, G.; Wong, W.-Y.; Poon, S.-Y.; Ye, C.; Lin, Z. *Adv. Funct. Mater.* **2009**, *19*, 531–544.
- (20) Spangler, C. W. *J. Mater. Chem.* **1999**, *9*, 2013–2020.
- (21) Marder, S. R.; Gorman, C. B.; Meyers, F.; Perry, J. W.; Bourhill, G.; Bredas, J.-L.; Pierce, B. M. *Science* **1994**, *265*, 632–635.
- (22) Perry, J. W. In *Nonlinear Optics of Organic Molecules and Polymers*; Nalwa, H. S., Miyata, S., Eds.; CRC Press: Boca Raton, FL, 1997; pp 813–840.
- (23) McClain, W. M. *Acc. Chem. Res.* **1974**, *7*, 129–135.
- (24) McKay, T. J.; Bolger, J. A.; Staromlynska, J.; Davy, J. R. *J. Chem. Phys.* **1998**, *108*, 5537–5541.
- (25) Staromlynska, J.; McKay, T. J.; Bolger, J. A.; Davy, J. R. *J. Opt. Soc. Am. B* **1998**, *15*, 1731–1736.
- (26) Ehrlich, J. E.; Wu, X. L.; Lee, I. Y. S.; Hu, Z. Y.; Röckel, H.; Marder, S. R.; Perry, J. W. *Opt. Lett.* **1997**, *22*, 1843–1845.
- (27) Kim, K. Y.; Shelton, A. H.; Drobizhev, M.; Makarov, N.; Rebane, A.; Schanze, K. S. *J. Phys. Chem. A* **2010**, *114*, 7003–7013.
- (28) Rogers, J. E.; Slagle, J. E.; Krein, D. M.; Burke, A. R.; Hall, B. C.; Fratini, A.; McLean, D. G.; Fleitz, P. A.; Cooper, T. M.; Drobizhev, M.; Makarov, N. S.; Rebane, A.; Kim, K.-Y.; Farley, R.; Schanze, K. S. *Inorg. Chem.* **2007**, *46*, 6483–6494.
- (29) Wong, W.-Y. *Coord. Chem. Rev.* **2005**, *249*, 971–997.

- (30) Wong, W.-Y.; Harvey, P. D. *Macromol. Rapid Commun.* **2010**, *31*, 671–713.
- (31) Wong, W.-Y.; Ho, C.-L. *Acc. Chem. Res.* **2010**, *43*, 1246–1256.
- (32) Sonogashira, K.; Fujikura, Y.; Yatake, T.; Toyoshima, N.; Takahashi, S.; Hagihara, N. *J. Organomet. Chem.* **1978**, *145*, 101–108.
- (33) D'Amato, R.; Furlani, A.; Colapietro, M.; Portalone, G.; Casalbani, M.; Falconieri, M.; Russo, M. V. *J. Organomet. Chem.* **2001**, *627*, 13–22.
- (34) Liu, Y.; Jiang, S.; Glusac, K.; Powell, D. H.; Anderson, D. F.; Schanze, K. S. *J. Am. Chem. Soc.* **2002**, *124*, 12412–12413.
- (35) Carlsson, M.; Eliasson, B. *Organometallics* **2006**, *25*, 5500–5502.
- (36) Davies, S. J.; Johnson, B. F. G.; Khan, M. S.; Lewis, J. J. *Chem. Soc.-Chem. Commun.* **1991**, 187–188.
- (37) Khan, M. S.; Davies, S. J.; Kakkar, A. K.; Schwartz, D.; Lin, B.; Johnson, B. F. G.; Lewis, J. J. *Organomet. Chem.* **1992**, *424*, 87–97.
- (38) Sonogashira, K.; Takahashi, S.; Hagihara, N. *Macromolecules* **1977**, *10*, 879–880.
- (39) Takahashi, S.; Kariya, M.; Yatake, T.; Sonogashira, K.; Hagihara, N. *Macromolecules* **1978**, *11*, 1063–1066.
- (40) Tour, J. M. *Chem. Rev.* **1996**, *96*, 537–554.
- (41) Schumm, J. S.; Pearson, D. L.; Tour, J. M. *Angew. Chem., Int. Ed.* **1994**, *33*, 1360–1363.
- (42) Wuts, P. G. M.; Greene, T. W. *Greene's Protective Groups in Organic Synthesis*; John Wiley & Sons: Hoboken, NJ, 2007.
- (43) Kukula, H.; Veit, S.; Godt, A. *Eur. J. Org. Chem.* **1999**, 277–286.
- (44) Keller, J. M.; Schanze, K. S. *Organometallics* **2009**, *28*, 4210–4216.
- (45) Liu, Y.; Jiang, S. J.; Glusac, K.; Powell, D. H.; Anderson, D. F.; Schanze, K. S. *J. Am. Chem. Soc.* **2002**, *124*, 12412–12413.
- (46) Silverman, E. E.; Cardolaccia, T.; Zhao, X.; Kim, K.-Y.; Haskins-Glusac, K.; Schanze, K. S. *Coord. Chem. Rev.* **2005**, *249*, 1491–1500.
- (47) Kim, K.-Y.; Schanze, K. S. *SPIE* **2006**, *6331*, 63310C.
- (48) Onitsuka, K.; Fujimoto, M.; Kitajima, H.; Ohshiro, N.; Takei, F.; Takahashi, S. *Chem.—Eur. J.* **2004**, *10*, 6433–6446.
- (49) Cooper, T. M.; Krein, D. M.; Burke, A. R.; McLean, D. G.; Rogers, J. E.; Slagle, J. E.; Fleitz, P. A. *J. Phys. Chem. A* **2006**, *110*, 4369–4375.
- (50) Cooper, T. M.; Hall, B. C.; McLean, D. G.; Rogers, J. E.; Burke, A. R.; Turnbull, K.; Weisner, A.; Fratini, A.; Liu, Y.; Schanze, K. S. *J. Phys. Chem. A* **2005**, *109*, 999–1007.
- (51) Cooper, T. M.; Krein, D. M.; Burke, A. R.; McLean, D. G.; Rogers, J. E.; Slagle, J. E. *J. Phys. Chem. A* **2006**, *110*, 13370–13378.
- (52) Vestberg, R.; Westlund, R.; Eriksson, A.; Lopes, C.; Carlsson, M.; Eliasson, B.; Glimsdal, E.; Lindgren, M.; Malmstrom, E. *Macromolecules* **2006**, *39*, 2238–2246.
- (53) Bruce, M. I.; Davy, J.; Hall, B. C.; van Galen, Y. J.; Skelton, B. W.; White, A. H. *Appl. Organomet. Chem.* **2002**, *16*, 559–568.
- (54) Beljonne, D.; Wittmann, H. F.; Kohler, A.; Graham, S.; Younus, M.; Lewis, J.; Raithby, P. R.; Khan, M. S.; Friend, R. H.; Bredas, J. L. *J. Chem. Phys.* **1996**, *105*, 3868–3877.
- (55) Glusac, K.; Kose, M. E.; Jiang, H.; Schanze, K. S. *J. Phys. Chem. B* **2007**, *111*, 929–940.
- (56) Wilson, J. S.; Chawdhury, N.; Al-Mandhary, M. R. A.; Younus, M.; Khan, M. S.; Raithby, P. R.; Kohler, A.; Friend, R. H. *J. Am. Chem. Soc.* **2001**, *123*, 9412–9417.
- (57) Wong, W.-Y.; Wang, X.-Z.; He, Z.; Djuricic, A. B.; Yip, C.-T.; Cheung, K.-Y.; Wang, H.; Mak, C. S. K.; Chan, W.-K. *Nat. Mater.* **2007**, *6*, 521–527.
- (58) Wong, W.-Y.; Wang, X.-Z.; He, Z.; Chan, K.-K.; Djuricic, A. B.; Cheung, K.-Y.; Yip, C.-T.; Ng, A. M.-C.; Xi, Y. Y.; Mak, C. S. K.; Chan, W.-K. *J. Am. Chem. Soc.* **2007**, *129*, 14372–14380.
- (59) Wong, W.-Y. *Macromol. Chem. Phys.* **2008**, *209*, 14–24.
- (60) Mei, J.; Ogawa, K.; Kim, Y. G.; Heston, N. C.; Arenas, D. J.; Nasrollahi, Z.; McCarley, T. D.; Tanner, D. B.; Reynolds, J. R.; Schanze, K. S. *ACS Appl. Mater. Interfac* **2009**, *1*, 150–161.
- (61) Zhao, X. Y.; Piliago, C.; Kim, B.; Poulsen, D. A.; Ma, B. W.; Unruh, D. A.; Frechet, J. M. J. *Chem. Mater.* **2010**, *22*, 2325–2332.
- (62) Goudreault, T.; He, Z.; Guo, Y.; Ho, C.-L.; Zhan, H.; Wang, Q.; Ho, K. Y.-F.; Wong, K.-L.; Fortin, D.; Yao, B.; Xie, Z.; Wang, L.; Kwok, W.-M.; Harvey, P. D.; Wong, W.-Y. *Macromolecules* **2010**, *43*, 7936–7949.
- (63) Rogers, J. E.; Hall, B. C.; Hufnagle, D. C.; Slagle, J. E.; Ault, A. P.; McLean, D. G.; Fleitz, P. A.; Cooper, T. M. *J. Chem. Phys.* **2005**, *122*, 214708.
- (64) Yang, Z.-D.; Feng, J.-K.; Ren, A.-M. *Inorg. Chem.* **2008**, *47*, 10841–10850.
- (65) Sheik-Bahae, M.; Said, A. A.; Van Stryland, E. W. *Opt. Lett.* **1989**, *14*, 955–957.
- (66) Sheik-Bahae, M.; Said, A. A.; Wei, T. H.; Hagan, D. J.; Van Stryland, E. W. *IEEE J. Quantum Electron.* **1990**, *26*, 760–769.
- (67) Shelton, A. H.; Schanze, K. S. *Unpublished results*; University of Florida: Gainesville, FL, 2010.
- (68) Makarov, N. S.; Drobizhev, M.; Rebane, A. *Opt. Express* **2008**, *16*, 4029–4047.
- (69) Xu, C.; Webb, W. W. *J. Opt. Soc. Am. B—Opt. Phys.* **1996**, *13*, 481–491.
- (70) Bhawalkar, J. D.; He, G. S.; Prasad, P. N. *Rep. Prog. Phys.* **1996**, *59*, 1041–1070.
- (71) Rumi, M.; Ehrlich, J. E.; Heikal, A. A.; Perry, J. W.; Barlow, S.; Hu, Z.; McCord-Maughon, D.; Parker, T. C.; Roedel, H.; Thayumanavan, S.; Marder, S. R.; Beljonne, D.; Bredas, J.-L. *J. Am. Chem. Soc.* **2000**, *122*, 9500–9510.
- (72) McKay, T. J.; Staromlynska, J.; Davy, J. R.; Bolger, J. A. *J. Opt. Soc. Am. B* **2001**, *18*, 358–362.
- (73) McKay, T. J.; Staromlynska, J.; Wilson, P.; Davy, J. J. *Appl. Phys.* **1999**, *85*, 1337–1341.
- (74) Glimsdal, E.; Eriksson, A.; Vestberg, R.; Malmstrom, E.; Lindgren, M.; Yeates, A. T., Ed.; SPIE: Bellingham, WA, 2005; Vol. 5934, p 59340N.
- (75) Lind, P.; Bostroem, D.; Carlsson, M.; Eriksson, A.; Glimsdal, E.; Lindgren, M.; Eliasson, B. *J. Phys. Chem. A* **2007**, *111*, 1598–1609.
- (76) Glimsdal, E.; Carlsson, M.; Kindahl, T.; Lindgren, M.; Lopes, C.; Eliasson, B. *J. Phys. Chem. A* **2010**, *114*, 3431–3442.
- (77) Chan, C. K. M.; Tao, C.-H.; Tam, H.-L.; Zhu, N.; Yam, V. W.-W.; Cheah, K.-W. *Inorg. Chem.* **2009**, *48*, 2855–2864.
- (78) Tao, C.-H.; Yang, H.; Zhu, N.; Yam, V. W.-W.; Xu, S.-J. *Organometallics* **2008**, *27*, 5453–5458.
- (79) Cooper, T. M.; Hall, B. C.; Burke, A. R.; Rogers, J. E.; McLean, D. G.; Slagle, J. E.; Fleitz, P. A. *Chem. Mater.* **2004**, *16*, 3215–3217.
- (80) Kim, K.-Y.; Schanze, K. S. *Unpublished work*; University of Florida: Gainesville, FL, 2004.
- (81) Zieba, R.; Desroches, C.; Chaput, F.; Carlsson, M.; Eliasson, B.; Lopes, C.; Lindgren, M.; Parola, S. *Adv. Funct. Mater.* **2009**, *19*, 235–241.